The Reduction of $[Fe(CO)_2L_2X_2]$ ($L = P(OMe)_3$, $P(OiPr)_3$, PEt_3; $X = Br$, I)—From Iron(II) to Iron(0) via Stable Iron(I) Intermediates

Helmut Kandler, Christine Gauss, Wolfgang Bidell, Stephan Rosenberger, Tobias Bürgi, Igor L. Eremenko, Dario Veghini, Olli Orama, Peter Burger, and Heinz Berke*

Abstract: The reduction of $[Fe(CO)_2L_2X_2]$ ($L = P(OMe)_3$, $X = Br$ (**1a**), I (**1b**); $L = P(OiPr)_3$, $X = Br$ (**2a**), I (**2b**); $L = PEt_3$, $X = Br$ (**3a**), I (**3b**)) with Zn in dioxane (**1a,b**–**2a,b**) or PhLi in ether (**3a,b**) led to formation of the corresponding dicarbonyl(halo)bis(phosphorus donor)iron(I) complexes ($L = P(OMe)_3$, $X = Br$ (**4a**), I (**4b**); $L = P(OiPr)_3$, $X = Br$ (**5a**), I (**5b**); $L = PEt_3$, $X = Br$ (**6a**), I (**6b**)). Slightly contaminated **5a,b** and pure **6a,b** were isolated as stable crystalline blue or blue-green complexes. Complexes **4a,b** were obtained, with only minor impurities, by comproportionation of **1a,b** and the dicarbonyl(halo)bis(trimethylphosphite)ferrate anions **7a,b** and characterized in THF solution. The comproportionation products **5a,b**–**6a,b** were obtained in high yields by reaction of **2a,b**–**3a,b** with the dinitrogen complexes **13**–**15**. Further reduction of **4a,b**–**6a,b** or exhaustive reduction of **1a,b**–**3a,b** with sodium amalgam or *t*BuLi in THF afforded the nonisolable dicarbonyl(halo)bis(phosphorus donor)ferrate(0) anions (**7a,b**–**9a,b**). The latter were characterized by acidification with trifluoroacetic acid or acetic acid yielding stable dicarbonyl (halo) hydridobis (phosphorus donor)iron(II) complexes ($L = P(OMe)_3$, $X = Br$ (**10a**), I (**10b**); $L = P(OiPr)_3$, $X = Br$ (**11a**), I (**11b**); $L = PEt_3$, $X = Br$ (**12a**), I (**12b**)). In the presence of N_2, **8a** was transformed into dinitrogen complex $[Fe(CO)_2\{P(OiPr)_3\}_2N_2]$ (**13**). With **9a,b** the reaction led to formation of $[Fe(CO)_2(PEt_3)_2N_2]$ (**14**) and $[\{Fe(CO)_2(PEt_3)_2\}_2(\mu\text{-}N_2)]$ (**15**). In solution at low temperature (−90 to 0 °C), the dinitrogen complexes **14** and **15** are in equilibrium with each other. Complexes **13**, **14**, and **15** were characterized by IR, ^1H, ^{13}C, ^{31}P, and ^{15}N NMR spectroscopy. The structures of **5a**, **6b**, **14**, and **15** were determined by X-ray diffraction studies.

Keywords
dinitrogen complexes · EPR spectroscopy · iron compounds · reductions

Introduction

Two-electron reductive replacement of two halides by various types of ligands is a versatile reaction step in organometallic chemistry. Normally very reactive intermediates analogous to carbenes are generated in this process, which can then undergo addition of neutral electron-donating ligands or oxidative addition of X–Y. A number mechanistic investigations have addressed the formation of intermediates generated by two consecutive one-electron transfers to a variety of transition-metal dihalide compounds.[1] These two steps can, however, not be distinguished mechanistically in all cases. For the reduction processes of iron complexes, only limited data are available.[2]

Recently, Cardaci et al. have published a method for the preparation of alkyl iron complexes:[2a] on reduction of Fe^{II} compounds it was postulated that reactive 16-electron species were formed, which underwent oxidative addition in situ with alkyl halides. Their interesting results prompted us to reinitiate our research in the area of Fe^0 dinitrogen complexes. In earlier publications we described a photochemical method for accessing these complexes.[3, 4]

In this paper we would like to report on the reduction of $[Fe^{II}(CO)_2L_2X_2]$ (L = phosphorus donor, X = Br, I) to give paramagnetic Fe^I complexes and then anionic Fe^0 transient intermediates $[Fe(CO)_2L_2X]^-$. Subsequent replacement of the halide ligand by dinitrogen resulted in the formation of the mono- or dinuclear dinitrogen complexes $[Fe(CO)_2L_2N_2]$ and $[\{Fe(CO)_2L_2\}_2(\mu\text{-}N_2)]$, respectively.[3, 4]

Results and Discussion

The reduction of complexes **1a,b**–**2a,b** with excess Zn in dioxane and of complexes **3a,b** with three equivalents of phenyllithium in ether proceeded with loss of one halogen substituent to afford the paramagnetic blue or green 17-electron iron(I) compounds **4a,b**–**6a,b** (Scheme 1). In the reduction of **1a,b** with Zn, some $[Fe(CO)_3\{P(OMe)_3\}_2]$ and $[Fe(CO)_2\{P(OMe)_3\}_3]$ were isolated as by-products, in addition to **4a,b**.[3a] While **5a,b** could be isolated in analytically pure form, **6a,b** were characterized as spectroscopically pure compounds.

When sodium amalgam in THF was used as the reducing agent and the reaction temperature was kept below −30 °C, the

[*] H. Berke, H. Kandler, C. Gauss, W. Bidell, S. Rosenberger, T. Bürgi, I. L. Eremenko, D. Veghini, O. Orama, P. Burger
Anorganisch-chemisches Institut, Universität Zürich
Winterthurerstr. 190, CH-8057 Zürich (Switzerland)
Telefax: Int. code + (1) 364-0191
e-mail: hberke@aci.unizh.ch

  0947-6539/95/0108-0541 $ 30.00+.25/0

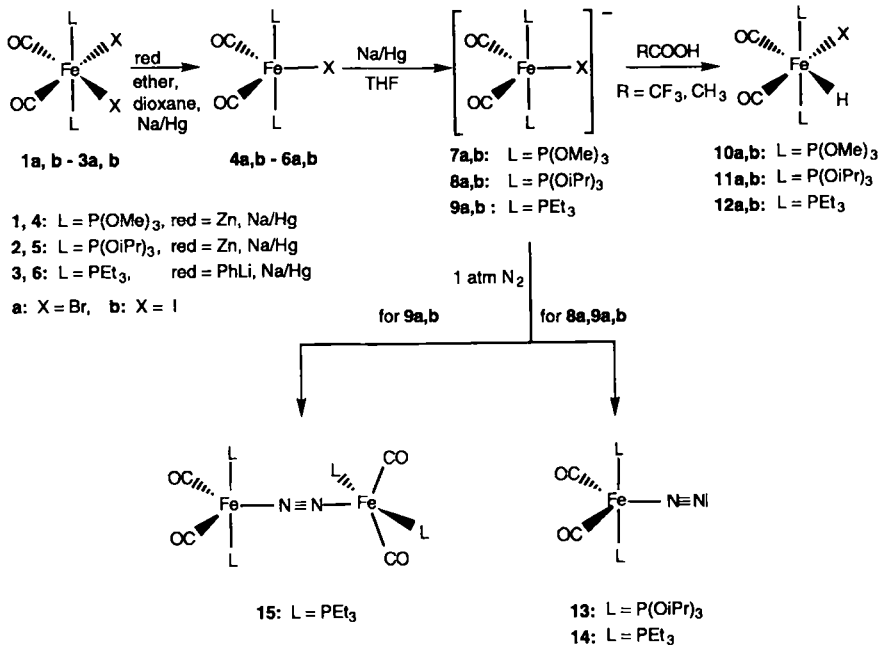

Scheme 1.

iron(I) complexes **4a,b–6a,b** were again obtained. However, at higher temperatures and with longer reaction times, two electrons were transferred to the iron(II) center and thermally labile Fe^0 compounds were formed (vide infra). Alternative and superior access to **4a,b–6a,b** was achieved through comproportionation. Thus, reaction of **1a,b** with the anions **7a,b** (vide infra) in THF at −30 °C (Scheme 2) yielded **4a,b** with only minute contamination with Fe^0 by-products. Owing to their thermal instability (even below 0 °C) and high solubility, **4a,b** could not be isolated in analytically pure form. Comproportionation of **2a,b** with **13** and **3a,b** with **15** (vide infra) was also found to be a superior route to the iron(I) complexes **5a,b** and **6a,b**, respectively. In these cases we were able to obtain crystalline **5a,b** and **6a,b**, which were oxygen-sensitive even in solid state.

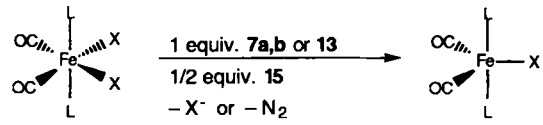

Scheme 2.

The structures of **4a,b–6a,b** were derived from X-ray diffraction studies (for **5a** and **6b**, Fig. 2) and from their spectroscopic data (Table 1). The IR spectra (ν_{CO} region) show two bands corresponding to a symmetric and an asymmetric stretch. In the derivatives **6a,b**, which contain more electron-rich phosphane ligands than **4a,b** and **5a,b**, these vibrations are shifted to lower wave numbers.

Table 1. Solution IR ($\tilde{\nu}$(CO)) and EPR Data of **4a,b–6a,b** (heptane).

	IR	EPR	
	$\tilde{\nu}$(CO) [cm^{-1}]	$\langle g \rangle$	$\langle A \rangle$ [G]
4a [a]	1995, 1926	2.062	34.5
4b [a]	1994, 1926	2.090	27.0
5a	1995, 1926	2.064	34.5
5b	1996, 1928	2.086	33.8
6a	1955, 1884	2.057	25.5
6b	1956, 1886	2.078	24.0

[a] Measured in THF.

The EPR spectra of **4a,b–6a,b** (Table 1) display triplet signals indicative of coupling with two equivalent ^{31}P nuclei. Larger $\langle g \rangle$ values were observed for the iodine derivatives. This is presumably due to the heavy-atom effect of iodine, which provides enhanced spin–orbit coupling. It should be noted, that shorter M–P bonds are in general observed for complexes with P = phosphite compared to P = phosphane.[5] This trend is also reflected in the X-ray crystal structures of **5a** (Fe–P(O*i*Pr)$_3$ = 2.206(2) Å) and **6b** (Fe–PEt$_3$ = 2.250(2) Å). Assuming a similar relation for **4a,b–5a,b** and **6a,b**, one can correlate the hyperfine coupling constants with the Fe–P bond lengths, that is, shorter Fe–P bonds lead to larger P coupling constants (Table 1). Compared with couplings of analogous P-centered phosphanyl radical ligands, the observed coupling in the complexes **4a,b–6a,b** is rather small.[6] It is worth mentioning that even smaller couplings of between 17 and 25 G have been determined for structurally related 17-electron iron complexes of the type $[Fe(CO)_2L_2L']^n$ (L = phosphorus donor, L′ = CO, $n = +1$; L′ = COX, $n = 0$).[1b, 7] This observation can be interpreted in terms of the fact that there is little orbital participation of phosphorus in the SOMO (singly occupied molecular orbital) and implies that the unpaired electron resides mainly in an orbital located in the equatorial atoms. Since the only spin-active isotope of iron, ^{57}Fe ($I = 1/2$), has a very low natural abundance (2.1%), no evidence for this assignment could be derived through additional Fe coupling.

An EHT (extended Hückel theory) calculation[8] was therefore conducted on the $[Fe(CO)_2(PH_3)_2I]$ model compound (with an idealized trigonal bipyramidal geometry) in order to provide further support for the proposed iron-centered radical. The calculation shows that the SOMO is basically an antibonding Fe–I orbital (see the $10a_1$ function in Fig. 3) with some admixture of the carbonyl groups. The SOMO is completely localized in the $Fe(CO)_2I$ plane and has therefore no coefficient on the phosphorus atoms. This would indeed confirm that the P coupling operates through spin polarization of doubly occupied MO's.

In general 17-electron radicals, such as $[Fe(CO)_4R]$ (R = acyl, H, alkyl), are thermally highly unstable and undergo transformation into di- or trinuclear species with concomitant metal–metal bond formation.[9] The higher stability in **4a,b–6a,b** demonstrates the important influence of the phosphorus donors and/or the halide substituents: the increased steric demand of the phosphorus donor in complexes **4a,b–6a,b**, presumably prevents the formation of halide-bridged species with or without metal–metal bonds. The complexes $[\{Ru(CO)_{4-x}L_xX\}_2]$ (L = phosphorus donor, X = Cl, Br) of the related higher homologous transition metal are apparently dimeric in the solid state and in solution.[10] The difference in behavior between the ruthenium and iron congeners is presumably best explained by the smaller covalent radius for the 3d transition metal, which would result in shorter Fe–Fe bonds. Thus, a dimeric Fe complex would be destabilized by enhanced

0947-6539/95/0108-0542 $ 30.00+.25/0 Chem. Eur. J. 1995, 1, No. 8

repulsion of the P ligands. It should be noted that a related methodology has been used for the design of persistent organic and, more recently, organometallic complexes.[11, 12] A prominent example is given by complexes of the type $[Re_2(CO)_{10-x}L_x]$, where, for L = phosphane with large Tolman cone angles, the persistent radicals $[Re(CO)_{5-x}L_x]$ are stable.[11c] Another very recent example has been published by Kubas et al. for $[W(CO)_3(PiPr_3)_2I]$.[12] For this complex it has also been proposed that the steric demand of the bulky phosphane substituents prevents dimerization. This suggests that the radical centers in **4a,b**–**6a,b** are sterically shielded or that the SOMOs are strongly delocalized. Cardaci et al. investigated the reduction of $[Fe(CO)_2L_2X_2]$ complexes and proposed, based on IR data, that the reduction products form trinuclear $[\{Fe(CO)_2L_2\}_3]$ species.[2a] The IR data presented resemble that for **4a,b**–**6a,b**, and we therefore propose that their compounds are also mononuclear 17-electron $[Fe(CO)_2L_2X]$ species.

Further reduction of **4a,b**–**6a,b** to Fe^0 complexes was accomplished with either Na/Hg or *t*BuLi (Scheme 1). The outcome of these reductions was, however, complicated by the fact that different reaction products were obtained when the reactions were carried under an argon or a dinitrogen atmosphere. Under argon, the reduction led to intermediates that were tentatively assigned to the anionic species $[Fe(CO)_2L_2X]^-$, based on the IR spectra, which display the $\tilde{\nu}$(CO) bands at lower wavenumbers than the values for the starting materials **4a,b**–**6a,b**, and the ^{31}P NMR spectra, which contain sharp singlets. It should be noted that electrochemical studies on other transition metal complexes provide evidence for such anionic species.[1c, d] Since attempts to isolate the thermally labile species $[Fe(CO)_2L_2X]^-$ by crystallization after cation exchange with $[AsPh_4]^+$ or $[Ph_3P{=}N{=}PPh_3]^+$ were unsuccessful, we sought to trap these intermediates as their corresponding hydride complexes by protonation. Dicarbonyl(halo)hydridobis(phosphorus donor)iron(II) compounds (L = $P(OMe)_3$, **10a,b**; L = $P(OiPr)_3$, **11a,b**; L = PEt_3, **12a,b**; Scheme 1) were indeed isolated in good yields by acidification of the reaction mixtures. The known complexes **11b**[4] and **12a,b**[13] were identified by comparison with spectroscopic data reported in the literature.

The reductions according to Scheme 1 took a slightly different course under an atmosphere of N_2 (1 atm). With **4a,b** (L = $P(OMe)_3$ and X = Br, I) and **5b** ($P(OiPr)_3$ and X = I) formation of the anionic species **7a,b** and **8b** was also observed. With **5a** (L = $P(OiPr)_3$, X = Br), however, the initially detected **8a** underwent substitution of the halide by N_2 to give the end-on dinitrogen complex $[Fe(CO)_2\{P(OiPr)_3\}_2(N_2)]$ (**13**). In the reduction of **6a,b**, we obtained a mixture of the η^1- and μ^2-dinitrogen compounds $[Fe(CO)_2(PEt_3)_2(N_2)]$ (**14**) and $[\{Fe(CO)_2(PEt_3)_2\}_2(\mu\text{-}N_2)]$ (**15**). We were, however, not able to observe the corresponding anionic intermediates **9a,b**. We assume that they are formed in the reduction process, since the low-temperature reaction of N_2 with **9a,b** generated under argon also led to **14**/**15** (Scheme 1).

It is interesting to note that for L = $P(OiPr)_3$ only the end-on compound **13** was observed within the limits of IR and NMR detection (−70 to 0 °C), while for L = PEt_3 a 20:1 ratio of **14**:**15** was detected in THF solution by ^{31}P NMR at −50 °C. Since the Tolman cone angles of $P(OiPr)_3$ and PEt_3 (130 and 132°, respectively)[14] are quite close, it is believed that steric factors are not responsible for this difference. This implies that the propensity to form μ-dinitrogen complexes is only influenced by the electronic properties of the phosphorus donors. It is known that coordination of N_2 to a metal center results in increased Lewis basicity of N_β in the resulting end-on N_2 complex.[15] This effect is expected to be more pronounced in **14** than in **13**, owing the presence of stronger electron-donating phosphane ligands in the former. However, the Lewis acidity of the $[Fe(CO)_2(PEt_3)_2]$ fragment, which adds to **14**, is lower than that of $[Fe(CO)_2(OiPr_3)_2]$. Hence, the formation of μ-N_2 species such as **15** may be considered to be the result of a subtle balance of the Lewis acid/base properties of the metal fragments.

Solutions of **14**/**15** have been generated earlier in our laboratories from $[Fe(CO)_3(PEt_3)_2]$ by photochemical substitution[3, 4] and were used in situ without complete characterization. The reductive route to **14**/**15** (Scheme 1) is superior and allowed us to isolate sizeable quantities (73% yield) and to characterize them by X-ray structure analysis and detailed spectroscopic investigations. Reductive conversions to **13** were nearly quantitative (^{31}P NMR integration). Recrystallization from hexane led to pure **13**; however, due to its high solubility in this solvent, the isolated yield was lowered to 57%. Because of their high thermal instability, chemical analyses of the dinitrogen complexes **13**–**15** could not be obtained. When required for further transformations (e.g., oxidative addition or substitution of N_2 by other ligands), the dinitrogen complexes **13**, **14**, and **15** are preferably obtained from **2b** and **3a,b** by reduction without prior isolation of **5b** and **6a,b** and used directly in solution.[3, 4]

Recrystallization of the mixture of **14**/**15** in ether gave yellow crystals of **15** with an overall yield of 58%. This result was somewhat surprising, since the ratio **14**:**15** in the low-temperature reaction mixtures was approximately 20:1 (vide supra). In solution, the μ-N_2 complex **15** apparently has a lower solubility than the end-on derivative **14**. Since **15** is isolated from this crystallization in a larger amount than was present in solution, this suggests that, even at low temperature, **14** and **15** are in equilibrium with each other. Hence, this conversion represents a nice example of a second-order transformation. A similiar observation was made for the dinuclear complex $[(tp^*IrPh_2)_2(\mu\text{-}N_2)]$ ($tp^* = HB(3,5\text{-}Me_2\text{-}pz)_3$),[16] which crystallizes from the solution of its mononuclear congener. When pentane was added to the supernatant solvent and the mixture chilled to −80 °C, orange crystals of **14** and yellow crystals of **15** were obtained in an approximate 1:1 ratio. Support for the proposed equilibrium between **14** and **15**, which is probably operating through scrambling of $[Fe(CO)_2(PEt_3)_2]$ fragments [Eq. (1a)], was then provided by the following experiments: When pure **15** was dissolved in $[D_8]$toluene at −90 °C under argon, only the resonances due to **15** could be observed. Upon warming of this sample to −80 °C, new resonances for **14** and the decomposition products, formed by reactions (1a) and (1c), were observed. When yellow crystals of **15** were dissolved under N_2 in $[D_8]$THF at −50 °C, a 20:1 ratio of **14**:**15** was immediately obtained, as shown by integration of the ^{31}P NMR spectrum. This process presumably occurs by generation of **14** with release of $[Fe(CO)_2(PEt_3)_2]$ fragments [Eq. (1a)], which are then trapped by N_2 [back reaction, Eq. (1b)].

$$\mathbf{15} \rightleftharpoons \mathbf{14} + [Fe(CO)_2(PEt_3)_2] \quad (1a)$$

$$\mathbf{14} \rightleftharpoons N_2 + [Fe(CO)_2(PEt_3)_2] \quad (1b)$$

$$[Fe(CO)_2(PEt_3)_2] \longrightarrow [Fe(CO)_3(PEt_3)_2] + [Fe(CO)_2(PEt_3)_3] + \ldots \quad (1c)$$

Degradation of **14** also sets in [Eq. (1b)] above 0 °C under Ar and above 10 °C under N_2. $[Fe(CO)_3(PEt_3)_2]$, $[Fe(CO)_2(PEt_3)_3]$, and other minute amounts of unidentified products were formed, presumably from the transient species $[Fe(CO)_2(PEt_3)_2]$ by some kind of ligand disproportionation reaction [Eq. (1c)].[3a] These results imply that, in the presence

of N_2, the rate of the back reaction of equilibrium (1b) is comparable with that of reaction (1c); this would also explain the higher overall thermal stability of the solution of **14/15** under N_2 (vide supra). Under the same conditions, solutions of **13** are somewhat less stable than those of **14/15**—at temperatures higher than 0°C a gradual decomposition to [Fe(CO)$_3${P(O*i*Pr)$_3$}$_2$] and [Fe(CO)$_2${P(O*i*Pr)$_3$}$_3$] was detected by ^{31}P NMR spectroscopy.

The comparison of the complexes described herein with other iron dinitrogen compounds[2b, 3, 4, 17, 18] shows that the thermal stability of such species increases in the presence of strongly electron-donating ligands. Thus, [Fe{bis(diethylphosphinoethane)}$_2$N$_2$][2b] is stable up to 150°C; this indicates that a higher degree of substitution at the phosphorus donor induces a stronger Fe–N_2 interaction.

The dinitrogen complexes **13**–**15** were further characterized by ^{15}N NMR spectroscopy. In order to obtain a better signal-to-noise ratio we sought to isotopically enrich **13**–**15** by exchange with $^{15}N_2$ (1 atm, 99% enriched). Indeed, we observed a smooth $^{14}N_2/^{15}N_2$ exchange in [D$_8$]THF over several hours. For **13**, this isotopomerization process was monitored at −40°C. Besides the singlet resonance at $\delta = -69.9$ for $^{15}N_2$,[19] the ^{15}N NMR spectrum (Fig. 1) exhibited two sets of

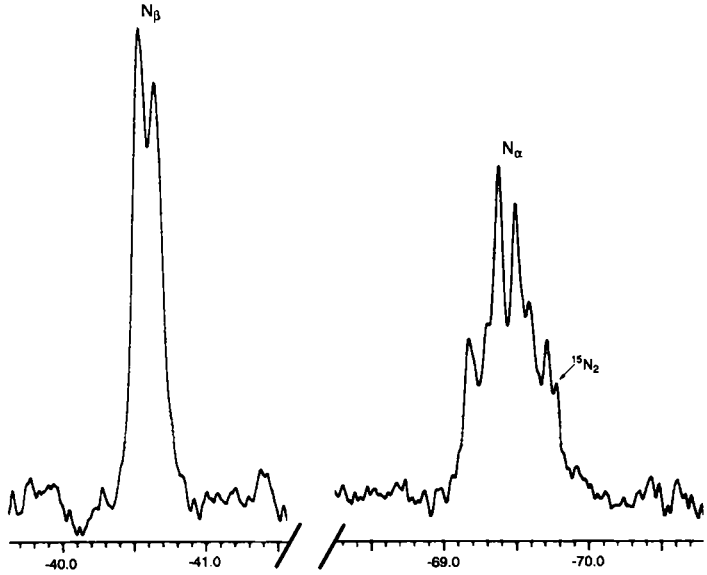

Fig. 1. ^{15}N NMR spectrum of **13** in [D$_8$]THF (ppm rel. CH_3NO_2).

resonances for the two chemically inequivalent ^{15}N nuclei. Under the assumption that $^2J_{PN} > {}^3J_{PN}$, the resonance at $\delta = -69.4$, which appears as a doublet of triplets ($J_{NN} = 3.3$, $J_{PN} = 6.3$ Hz), is assigned to the nitrogen atom bound to the iron center (N_α). For N_β a doublet is observed at $\delta = -40.6$. A $^{14}N_2/^{15}N_2$ exchange process was also observed for **14** in [D$_8$]THF at −10°C. In the ^{15}N NMR spectrum we could not detect resonances for complex **15**. This may be due to a) the reduced solubility of **14/15** compared to **13** and b) to the low equilibrium concentration of **15** (vide supra). Explanation a) would also account for the unresolved multiplet patterns at $\delta = -62.1$ (N_α) and −39.7 (N_β), which were tentatively assigned based on the ^{15}N NMR chemical shifts of **13**.

The low temperature solution IR spectra (0°C, 2200–1800 cm^{-1}) of **13** and **14** in hexane or THF showed three bands, which were assigned as $\nu(N_2)$, ν_s(CO), and ν_{as}(CO). The $\nu(N_2)$ bands appear in the absorption range observed for other mononuclear end-on N_2 iron complexes[20] ($\tilde{\nu}(N_2) = 2141$ cm^{-1} for **13** and 2097 cm^{-1} for **14**). The solid-state IR spectrum of **15** was obtained in a fluorocarbon mull. Because **15** is completely insoluble in this medium, the conversion into **14** was apparently prevented—only three absorption bands were detected in the IR spectrum. As expected from the idealized D_{2d} molecular symmetry of **15** (vide infra) and by comparison with dinuclear carbonyl complexes of the same symmetry,[21] we assigned these three absorption bands to $\tilde{\nu}$(CO) streching frequencies.

Structure determinations of 5a, 6b, 14, and 15: Stable mononuclear Fe^I complexes are very rare.[7a, 22] Therefore, we sought to explore the solid-state structures of representative examples from the **4a,b**–**6a,b** series by X-ray diffraction studies.

The structures of **5a** and **6b** (Fig. 2, Table 2) reveal pseudo trigonal-bipyramidal coordination geometries with the phosphane substituents in axial and the CO and the halide moieties in equatorial positions. The bond lengths around the paramagnetic iron centers compare well with those of related complexes with closed-shell configurations.[5] The angles between the carbonyl groups (∢OC-Fe-CO) are remarkably small (102.6 and 97.5° for **5a** and **6b**, respectively). In order to understand this structural phenomenon we carried out EHT calculations.

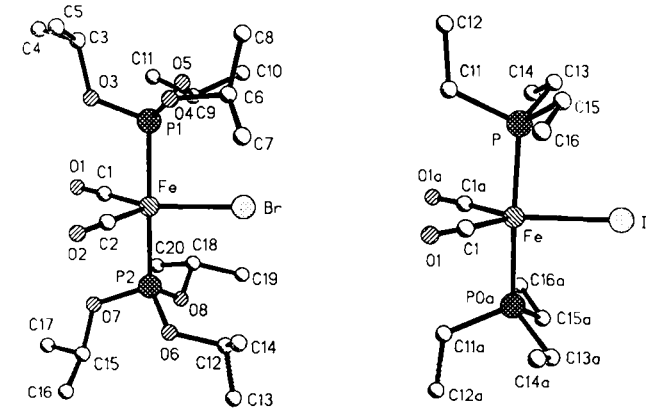

Fig. 2. Structures of **5a** (left) and **6b** (right).

Table 2. Selected bond lengths [Å] and angles [°] of **5a** and **6b**.

5a		**6b**	
Fe–Br	2.423(2)	Fe–I	2.610(1)
Fe–C(1)	1.794(6)	Fe–C(1)	1.774(7)
Fe–C(2)	1.795(7)	Fe–C(1a)	1.777(7)
Fe–P(1)	2.206(2)	Fe–P	2.250(2)
Fe–P(2)	2.203(2)	Fe–P(a)	2.245(2)
C(1)–O(1)	1.127(7)	C(1)–O(1)	1.140(9)
C(2)–O(2)	1.153(9)		
Br-Fe-P(1)	89.9(1)	I-Fe-P	88.6(1)
Br-Fe-P(2)	89.4(1)	I-Fe-P(a)	88.7(1)
Br-Fe-C(1)	134.0(2)	I-Fe-C(1)	131.4(3)
Br-Fe-C(2)	123.4(2)	I-Fe-C(1a)	131.1(3)
P(1)-Fe-P(2)	178.7(1)	P-Fe-P(a)	177.2(1)
P(1)-Fe-C(1)	90.1(2)	P-Fe-C(1)	90.3(2)
P(1)-Fe-C(2)	90.7(2)	P-Fe-C(1a)	91.6(2)
P(2)-Fe-C(1)	89.6(2)	P(a)-Fe-C(1)	91.6(2)
P(2)-Fe-C(2)	90.6(2)	P(a)-Fe-C(1a)	90.4(2)
C(1)-Fe-C(2)	102.6(3)	C(1)-Fe-C(1a)	97.5(5)
Fe-C(1)-O(1)	178.6(6)	Fe-C(1)-O(1)	176.0(7)
Fe-C(2)-O(2)	178.1(5)		

0947-6539/95/0108-0544 $ 30.00+.25/0 Chem. Eur. J. 1995, 1, No. 8

EHT optimizations of the OC-Fe-CO angle in model complexes $[Fe(CO)_2(PH_3)_2X]$ (X = Br, I) gave total energy minima at 113 and 114°, respectively. Although the experimental and the calculated angles are not very close, our computations show that there is a tendency for such molecules to adopt an equatorial carbonyl angle smaller than 120°.

From the orbital correlation diagram of $[Fe(CO)_2(PH_3)_2I]$ in Figure 3, it can be seen that two orbitals are responsible for the major energetic changes: $7b_1$ (the SOMO) and $10a_1$. The correlation line of $7b_1$ decreases energetically and flattens somewhat

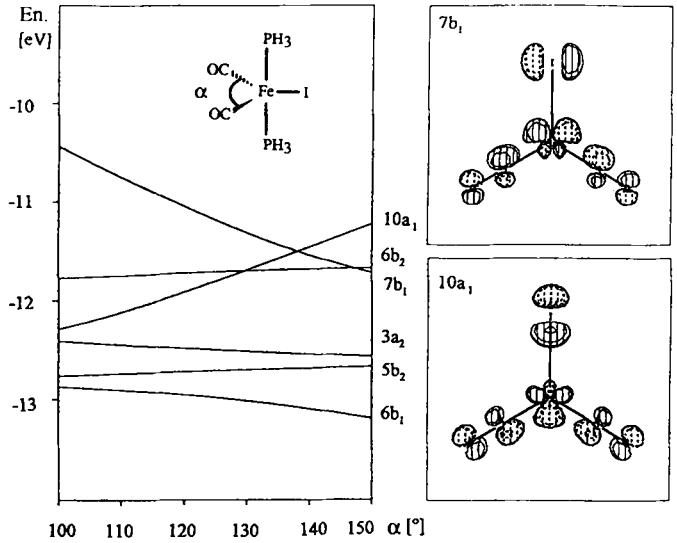

Fig. 3. Left: Orbital correlation diagram for changes in the $Fe(CO)_2$ angle α of $[Fe(CO)_2(PH_3)_2I]$, calculated from CACAO [8]. Right: CACAO orbital plots of the $7b_2$ and $10a_1$ functions of $[Fe(CO)_2(PH_3)_2I]$ in the $Fe(CO)_2I$ plane.

toward larger CO angles. The $10a_1$ curve increases in energy and becomes slightly steeper at about 115°. From the orbital plots of $7b_1$ and $10a_1$ in Figure 3, we derive that $7b_1$ is mainly σ antibonding in character between the CO groups and the metal. The $10a_1$ orbital principally consists of π-type Fe–CO bonding interaction. The counteracting angular dependency of these Fe–CO interactions leads to a quite shallow energy curve with a minimum at 142° when the two orbitals are each occupied by two electrons. This orbital occupancy mimics the electronic distribution in the anions **7–9**. In the radical $[Fe(CO)_2(PH_3)_2I]$, $7b_1$ is occupied by just one electron; this leads to a smaller $7b_1$ contribution to the total energy of this molecule and consequently to an energy minimum dominated by the influence of $10a_1$, that is, at smaller CO angles.

The preference of the N_2 to bind end-on in some complexes and as μ^2 bridging ligand in others is not yet fully understood. For an explanation based on stereoelectronic arguments,[23] structural data on related end-on and μ^2 complexes are required. To our knowledge, data of this kind is only available for coordination compounds $[Ru(NH_3)_5N_2]^{2+}$[24] and $[\{Ru(NH_3)_5\}_2N_2]^{4+}$.[25] We therefore carried out X-ray structure determinations on **14** and **15** in order to establish differences in the ligating properites of η^1- and μ^2-N_2 for this pair of organometallic derivatives.

The structure of **14** reveals a pseudo trigonal-bipyramidal coordination with only minor angular distortions from the ideal geometry. The distances between iron and the iron-bound atoms lie in the expected range (Fig. 4 and Table 3).[5, 26]

Complex **15** contains two iron centers coordinated as trigonal bipyramids, which are linked by the μ-N_2 bridge (Fig. 5). The iron fragments adopt a staggered conformation with respect to each other, which is presumably the minimum-energy conformation, in terms of electronic and steric considerations.[3a]

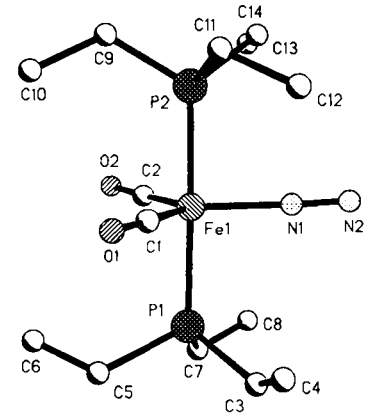

Fig. 4. Structure of **14**.

Complexes **14** and **15** contain structurally very similar $[Fe(CO)_2(PEt_3)_2]$ fragments (Table 3) (i.e., the angles and bond lengths are very similar). The Fe–N and N≡N bond lengths of **14** and **15** fall within the range determined for other first-row transition-metal dinitrogen complexes.[20, 27] The bond lengths also compare well with those of $[\{Fe(CO)_2[P(OMe)_3]_2\}_2(\mu\text{-}N_2)]$.[3a] While the Fe–N bond lengths of **14** and **15** are essentially identical within their standard deviations, the N–N separation in **15** seems to be somewhat longer. Because two metal centers are attached to the N_2 ligand in **15**, there might be a stronger charge transfer into the π^*_{NN} orbitals, which causes an elongation of the N–N bond.

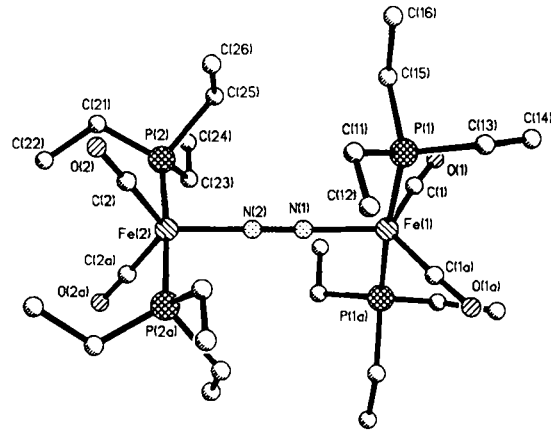

Fig. 5. Structure of **15**.

Table 3. Selected bond lengths [Å] and angles [°] of **14** and **15**.

14		**15**	
Fe(1)–P(1)	2.232(7)	Fe(1)–P(1)	2.224(3)
Fe(1)–P(2)	2.225(7)	Fe(2)–P(2)	2.207(6)
Fe(1)–N(1)	1.853(22)	Fe(1)–N(1)	1.867(13)
		Fe(2)–N(2)	1.890(16)
Fe(1)–C(1)	1.732(22)	Fe(1)–C(1)	1.747(16)
Fe(1)–C(2)	1.713(22)	Fe(2)–C(2)	1.726(11)
C(1)–O(1)	1.217(28)	C(1)–O(1)	1.162(20)
C(2)–O(2)	1.192(31)	C(2)–O(2)	1.172(14)
N(1)–N(2)	1.078(30)	N(1)–N(2)	1.134(21)
P(1)-Fe(1)-P(2)	175.0(3)	P(1)-Fe(1)-P(1a)	174.4(2)
		P(2)-Fe(2)-P(2a)	176.8(2)
N(1)-Fe(1)-C(1)	119.7(9)	N(1)-Fe(1)-C(1)	118.8(5)
N(1)-Fe(1)-C(2)	117.5(9)	N(2)-Fe(2)-C(2)	119.1(4)
C(1)-Fe(1)-C(2)	122.8(10)	C(1)-Fe(1)-C(1a)	122.3(9)
		C(2)-Fe(2)-C(2a)	121.0(9)
Fe(1)-N(1)-N(2)	178.7(20)	Fe(1)-N(1)-N(2)	180.0(1)
		Fe(2)-N(2)-N(1)	180.0(1)
Fe(1)-C(1)-O(1)	178.6(15)	Fe(1)-C(1)-O(1)	174.0(13)
Fe(1)-C(2)-O(2)	176.3(19)	Fe(2)-C(2)-O(2)	176.5(12)
P(1)-Fe(1)-N(1)	92.6(7)	P(1)-Fe(1)-N(1)	92.8(1)
P(2)-Fe(1)-N(1)	89.6(7)	P(2)-Fe(2)-N(2)	91.6(1)

Summary and Conclusions

The two-electron reduction of metal dihalide compounds $[L_nMX_2]$ is a widely used reaction in organometallic chemistry and affords $[L_nML']$ complexes in the presence of a further ligand L' [Eq. (2)]. Our investigations on the reduction

$$[L_nMX_2] \xrightarrow[+L']{2e^-} [L_nML'] + 2X^- \quad (2)$$

of $[Fe(CO)_2L_2X_2]$ (L = phosphorus donor, X = halide) have demonstrated for the first time the stepwise nature of such processes by isolation of the one-electron reduction products, namely, the pseudo trigonal-bipyramidal 17-electron compounds $[Fe(CO)_2L_2X]$. Subsequent reduction leads to $[Fe(CO)_2L_2X]^-$, in which the X^- ligand may be substituted by N_2. Interestingly, for the system with L = PEt_3 different binding modes of the N_2 ligand have been observed in the mono- and dinuclear species $[Fe(CO)_2(PEt_3)_2N_2]$ and $[\{Fe(CO)_2(PEt_3)_2\}_2(\mu\text{-}N_2)]$, in solution as well as in the solid state. In contrast, the $[Fe(CO)_2\{P(OiPr)_3\}_2]$ fragment only forms the end-on N_2 species. This difference in the binding capability of such $[Fe(CO)_2L_2]$ fragments is apparently related to the different donor properties of the phosphorus ligands and reveals a great potential for chemical tuning of such carbenoid $[Fe(CO)_2L_2]$ units, especially with regard to the possibility of facile changes in oxidation states.

Experimental Procedure

General: All preparations and manipulations were carried out under an atmosphere of dry dinitrogen or, if stated, under argon by conventional Schlenk techniques. Solvents were dried and freshly distilled before use. IR spectra were recorded on a Biorad FTS-45 instrument. MS spectra were run on a Finnigan MAT-8230 mass spectrometer. ^1H and $^{13}C\{^1H\}$ NMR spectra were recorded on a Varian Gemini-200 instrument operating at 200 and 50.3 MHz, respectively (δ (ppm rel. TMS), J in Hz), and $^{31}P\{^1H\}$ and $^{15}N\{^1H\}$ NMR spectra on a Varian Gemini-300 spectrometer at 121.5 and 30.4 MHz, respectively (δ: ppm rel. H_3PO_4 and CH_3NO_2, respectively).

Materials: PhLi, *t*BuLi, trifluoroacetic acid, and acetic acid were purchased from commercial suppliers. $[Fe(CO)_2L_2X_2]$ (L = $P(OMe)_3$, $P(OiPr)_3$, PEt_3; X = Br, I) were prepared according to literature procedures [28]. Column chromatography was performed with silica gel 60 from Merck, Darmstadt (Germany). Alumina (Alox 90, Merck) was degassed and Celite was dried and degassed prior to use.

Preparation of $[Fe(CO)_2\{P(OMe)_3\}_2X]$ (X = Br, 4a; X = I, 4b):
Reduction method: The reduction of $[Fe(CO)_2\{P(OMe)_3\}_2X_2]$ (**1a,b**, X = Br, I) (1.0 mmol) with Zn dust (0.65 g, 10 equiv) in dioxane (75 mL) at r.t. yielded a blue-green solution of **4a,b** (reaction time < 1 h). After filtration of the Zn dust, the solution contained greater quantities of impurities than obtained by the comproportionation method.
Comproportionation method: **1a,b** (1.6 mmol) was added in small portions to a solution of $[Fe(CO)_2\{P(OMe)_3\}_2X]^-$ (**7a,b**, X = Br, I) in THF (100 mL) at −30 °C, obtained by reduction of **1a,b** (2 mmol) with Na/Hg as described below. A blue-green color evolved, and the solution of **4a,b** was reduced in volume at −20 °C. Cold heptane was added and the volume of the reaction mixture was reduced in vacuo. NaX (X = Br, I) precipitated from the resulting heptane solution and was filtered off over Celite at low temperature ($T \leq -20$ °C). Products **4a,b** were identified by IR and EPR spectroscopy from these solutions (Table 1). Repeated attempts to isolate **4a,b** failed.

Preparation of $[Fe(CO)_2\{P(OiPr)_3\}_2X]$ (X = Br, 5a; X = I, 5b):
Reduction method: A solution of $[Fe(CO)_2\{P(OiPr)_3\}_2X_2]$ (X = Br, I, **2a,b**) (1.0 mmol) in dioxane (75 mL) was stirred with zinc dust (0.65 g, 10 mmol) at r.t. for 2 h. The reaction progress was monitored by IR spectroscopy. The intensely colored solution was filtered over alumina, and the filtrate evaporated to dryness. The residue was extracted into a minimum amount of hexane. The resulting solutions of **5a,b** were left to crystallize at −80 °C. **5a**: 0.69 g of **2a** yielded 0.30 g (50%) of blue crystals, containing $[Fe(CO)_3\{P(OiPr)_3\}_2]$ and $[Fe(CO)_2\{P(OiPr)_3\}_3]$ as minor impurities. **5b**: 0.78 g of **2b** yielded 0.30 g (46%) of green crystals. The IR spectrum of **5b** showed a slight contamination from $[Fe(CO)_3\{P(OiPr)_3\}_2]$ and $[Fe(CO)_2\{P(OiPr)_3\}_3]$. Repeated attempts to remove these by-products from **5a,b** resulted in further decomposition.
Comproportionation method: A yellow solution of $[Fe(CO)_2\{P(OiPr)_3\}_2N_2]$ (**13**) (1.11 g, 2.0 mmol), prepared as described below, in hexane (50 mL) was added to a solution of **2a,b** (2.0 mmol) in hexane (50 mL) at −20 °C. The reaction mixture was allowed to warm up to 0 °C, and a blue (X = Br) or green color (X = I) evolved. After 2 h the resulting solutions were concentrated and left to crystallize at −80 °C (IR and EPR data of **5a,b** see Table 1).
5a: 1.38 g of **2a** yielded 2.16 g (89%) of blue crystals. MS (70 eV, EI): *m/z* (%): 607 (16) $[M^+]$, 551 (70) $[M^+-2CO]$, 472 (63) $[Fe\{P(OiPr)_3\}_2^+]$, 343 (100) $[Fe\{P(OiPr)_3\}Br^+]$, 208 (55) $[P(OiPr)_3^+]$; $C_{20}H_{42}BrFeO_8P_2$ (608.3): calcd 39.49, H 6.96; found C 39.43, H 6.97.
5b: 1.56 g of **2b** yielded 2.38 g (91%) of green crystals. MS (70 eV, EI): *m/z* (%) = 655 (15) $[M^+]$, 599 (55) $[M^+-2CO]$, 472 (40) $[Fe\{P(OiPr)_3\}_2^+]$, 391 (60) $[Fe\{P(OiPr)_3\}Br^+]$, 208 (20) $[P(OiPr)_3^+]$; $C_{20}H_{42}FeIO_8P_2$ (655.3): calcd C 36.66, H 6.46, Fe 8.52; found C 36.75, H 6.43, Fe 8.73.

Preparation of $[Fe(CO)_2(PEt_3)_2X]$ (X = Br, 6a; X = I, 6b):
Reduction method: A suspension of $[Fe(CO)_2(PEt_3)_2X_2]$ (X = Br, I, **3a,b**) (1.4 mmol) in ether (100 mL) was cooled to −40 °C. A solution of PhLi in ether (1.9 M, 2.2 mL, 4.2 mmol) was added. After 1 h of stirring, the solution was filtered over Celite. The green filtrate was evaporated to dryness, and the residue extracted with hexane. Crystallization at −80 °C yielded the green complexes **6a** or **6b** with minor impurities (IR spectroscopy). **6a**: 0.71 g (1.4 mmol) of **3a** yielded 0.12 g (20%). **6b**: 0.84 g (1.4 mmol) of **3b** yielded 0.51 g (77%).
Comproportionation method: $[\{Fe(CO)_2(PEt_3)_2\}_2(\mu\text{-}N_2)]$ (**15**) (0.36 g, 0.5 mmol), prepared as described below, was dissolved in THF (25 mL) at −50 °C. The resulting yellow solution was added to a solution of **3a,b** (1.0 mmol) in THF. Slow warming to 0 °C within 3 h resulted in the formation of a green solution. Evaporation of the solvent, extraction with hexane, and crystallization at −80 °C yielded **6a,b** (for IR and EPR data see Table 1).
6a: 0.51 g of **3a** yielded 0.72 g (84%). MS (70 eV, EI): *m/z* (%): 427 (3) $[M^+]$, 371 $[M^+-2CO]$, 292 $[Fe(PEt_3)_2^+]$, 253 (100) $[Fe(PEt_3)Br^+]$, 118 $[PEt_3^+]$; $C_{14}H_{30}BrFeO_2P_2$ (428.1): calcd C 39.28, H 7.06, Fe 13.05; found C 38.36, H 6.76, Fe 13.02.
6b: 0.60 g (1.0 mmol) of **3b** yielded 0.83 g (87%). MS (70 eV, EI): *m/z* (%): 475 (10) $[M^+]$, 419 $[M^+-2CO]$, 301 (100) $[Fe(PEt_3)I^+]$, 292 $[Fe(PEt_3)_2^+]$, 118 $[PEt_3^+]$; $C_{14}H_{30}IFeO_2P_2$ (475.1): calcd C 35.39, H 6.36, Fe 11.75; found C 36.03, H 6.42, Fe 11.83.

Preparation of the $[Fe(CO)_2L_2X]^-$ complexes 7a (L = $P(OMe)_3$, X = Br), 7b (L = $P(OMe)_3$, X = I), and 8b (L = $P(OiPr)_3$, X = I): A solution of $[Fe(CO)_2L_2X_2]$ (L = $P(OMe)_3$, X = Br (**1a**), I (**1b**); L = $P(OiPr)_3$, X = I (**2b**)) (1.5 mmol) in THF (100 mL) was vigorously stirred with sodium amalgam (< 1% ca. 10 mmol Na) at ca −25 °C. After 2–3 h (IR monitoring) the supernatant suspension was transferred to a frit through a canula and filtered over Celite. The orange-red solution obtained contained the complexes **7a,b** or **8b** with only minor impurities (^{31}P NMR spectroscopy).
7a: $^{31}P\{^1H\}$ NMR ([D$_8$]THF, −20 °C): δ = 198.6; IR (THF): $\tilde{\nu}$ = 1881, 1817 cm^{-1} (2 × C=O). Above 0 °C slow decomposition sets in with formation of $[Fe(CO)_3\{P(OMe)_3\}_2]$ and $[Fe(CO)_2\{P(OMe)_3\}_3]$.
7b: $^{31}P\{^1H\}$ NMR (C_6D_6/THF, r.t.): δ = 198.4; IR (THF): $\tilde{\nu}$ = 1883, 1819 cm^{-1} (2 × C=O). The THF solution is stable at r.t.
8b: $^{31}P\{^1H\}$ NMR (C_6D_6/THF, r.t.): δ = 187.2; IR (THF): $\tilde{\nu}$ = 1872, 1811 cm^{-1} (2 × C=O). THF solutions are stable at r.t.

Preparation of $[Fe(CO)_2\{P(OiPr)_3\}_2Br]^-$ (8a): A solution of $[Fe(CO)_2\{P(OiPr)_3\}_2Br_2]$ (**2a**) (1.03 g, 1.5 mmol) in THF (100 mL) was cooled to −80 °C. A solution of *t*BuLi in hexane (1.4 M, 2.15 mL, 3.0 mmol) was added under an atmosphere of argon. The orange-yellow solution obtained contained the thermally unstable complex **8a**. **8a**: $^{31}P\{^1H\}$ NMR ([D$_8$]THF/THF, −50 °C): δ = 194.4; IR (THF): $\tilde{\nu}$ = 1879, 1812 cm^{-1} (2 × C=O).

Preparation of the $[Fe(CO)_2L_2(H)(X)]$ complexes 10a (L = $P(OMe)_3$, X = Br), 10b (L = $P(OMe)_3$, X = I), and 11b (L = $P(OiPr)_3$, X = I): Trifluoroacetic acid (80 μL, 1.0 mmol) was added to a THF solution of **7a,b** or **8b** (1.0 mmol), prepared as described above. The solvent was removed in vacuo, and oily residues were left behind. Extraction with hexane (10 mL) was followed by column chromatography on silica. Elution of the orange-yellow or orange band, concentration of the solvent, and crystallization at −30 °C afforded the corresponding compounds **10a,b** and **11b**. **11b** was characterized by comparison with spectroscopic data reported earlier [4].
10a: Column chromatography at 20 °C and elution with hexane/ether (10:1). Yield 0.44 g (66%). ^1H NMR (C_6D_6, r.t.): δ = −6.21 (t, J_{PH} = 60.2, Fe*H*), 3.57 (t, J_{PH} = 5.7, OC*H*$_3$); $^{13}C\{^1H\}$ NMR (C_6D_6, r.t.): δ = 53.2 (t, J_{PC} = 17.3, O*C*H$_3$), 211.9 (t, J_{PC} = 35.0, *C*O); $^{31}P\{^1H\}$ NMR (C_6D_6, r.t.): δ = 165.3; IR (hexane): $\tilde{\nu}$ = 2042, 1994 cm^{-1} (2 × C=O); MS (70 eV, EI): *m/z* (%): 383 $[M^+-2CO-H]$, 360 $[M^+-HBr]$, 332 $[M^+-2CO-HBr]$, 304 (100) $[FeLH^+]$; $C_8H_{19}BrFeO_8P_2$ (440.1): calcd C 21.79, H 4.34, Fe 12.67; found C 21.52, H 4.38, Fe 11.16.
10b: Column chromatography at 20 °C and elution with hexane/ether (10:1). Yield 0.44 g (90%). ^1H NMR (C_6D_6, r.t.): δ = −7.25 (t, J_{PH} = 60.6, Fe*H*) 3.52

0947-6539/95/0108-0546 $ 30.00+.25/0 Chem. Eur. J. 1995, 1, No. 8

(t, J_{PH} = 5.8, OCH_3); $^{13}C\{^1H\}$ NMR (C_6D_6, r.t.): δ = 53.6 (t, J_{PC} = 2.5, OCH_3), 207.6 (t, J_{PC} = 18.3, *CO*), 212.9 (t, J_{PC} = 34.7, *CO*); $^{31}P\{^1H\}$ NMR (C_6D_6, r.t.): δ = 168.0; IR (hexane): $\tilde{\nu}$ = 2040, 1992 cm^{-1} (2 × C≡O); MS (70 eV, EI): *m/z* (%): 488 (15) [M^+], 460 (1) [M^+–CO], 432 (20) [M^+–2CO], 360 (35) [M^+–HI], 332 (25) [M^+–CO–HI], 307 (40) [M^+–2CO–$P(OCH_3)_3$], 304 (60) [M^+–2CO–HI], 180 (15) [$FeP(OCH_3)_3^+$], 165 (5) [$FeP(OCH_3)_3^+$–CH_3], 135 (5) [$FeP(OCH_3)_2^+$–CH_3], 125 (25) [$P(OCH_3)_3^+$]; $C_8H_{19}FeIO_8P_2$ (487.9): calcd C 19.69, H 3.93, Fe 11.45; found C 19.85, H 3.96, Fe 11.16.

11b: Column chromatography (silica) at 20 °C and elution with hexane/ether (10:1). Yield 0.56 g (85%). ^1H NMR (C_6D_6, r.t.): δ = –6.69 (t, J_{PH} = 60.4, Fe*H*), 1.29 (m, $OCH(CH_3)_2$), 5.08 (m, $OCH(CH_3)_2$); $^{13}C\{^1H\}$ NMR (C_6D_6, r.t.): δ = 24.2 (s, $OCH(CH_3)_2$), 71.8 (s, $OCH(CH_3)_2$), 208.2 (t, J_{PC} = 19.5, *CO*), 214.3 (t, J_{PC} = 35.0, *CO*); $^{31}P\{^1H\}$ NMR (C_6D_6) r.t.): δ = 156.3; IR (hexane): $\tilde{\nu}$ = 2036, 1989 cm^{-1} (2 × C≡O); MS (70 eV, EI): *m/z* (%): 656 (5) [M^+], 628 (1) [M^+–CO], 600 (10) [M^+–2CO], 596 (10) [M^+–$HOCH(CH_3)_2$, 528 (10) [M^+–HI], 500 (5) [M^+–CO–HI], 473 (100) [M^+–2CO–I], 391 (20) [M^+–2CO–$P\{OCH(CH_3)_2\}_3$], 265 (15) [$FeP(OCH(CH_3)_2\}_3^+$], 209 (40) [$P\{OCH(CH_3)_2\}_3^+$]: $C_{20}H_{43}FeIO_8P_2$ (656.3): calcd C 36.60, H 6.60, Fe 8.51; found C 36.70, H 6.92, Fe 8.51.

Preparation of the $[Fe(CO)_2L_2(H)(X)]$ complexes 11a (L = $P(OiPr)_3$, X = Br), 12a (L = $P(Et)_3$, X = Br), and 12b (L = $P(Et)_3$, X = I): $[Fe(CO)_2L_2X_2]$ (L = $P(OiPr)_3$, X = Br (**2a**); L = $P(Et)_3$, X = Br (**3a**), I (**3b**)) (1.0 mmol) was reduced under an atmosphere of argon as described above for **8a**. Acetic acid (60 μL, 1.0 mmol) was added at –80 °C, and the reaction mixture was allowed to warm up to r.t. The solvent of the yellow solution was removed in vacuo. Extraction into a minimum amount of hexane was followed by crystallization at –30 °C.

11a: Yield: 0.51 g (83%). ^1H NMR (C_6D_6, r.t.): δ = –5.62 (t, J_{PH} = 60.7, Fe*H*), 1.27 (d, J_{PH} = 6.2, diastereotopic $OCH(CH_3)_2$), 1.34 (d, J_{PH} = 6.2, diastereotopic $OCH(CH_3)_2$), 5.13 (m, $OCH(CH_3)_2$); $^{13}C\{^1H\}$ NMR (C_6D_6, r.t.): δ = 24.2 (s, diastereotopic $OCH(CH_3)_2$), 24.2 (s, diastereotopic $OCH(CH_3)_2$), 71.1 (t, J_{PC} = 3.0, $OCH(CH_3)_2$), 208.2 (t, J_{PC} = 18.5, *CO*), 213.1 (t, J_{PC} = 34.5, *CO*); $^{31}P\{^1H\}$ NMR (C_6D_6, r.t.): δ = 154.3; IR (hexane): $\tilde{\nu}$ = 2038, 1989 cm^{-1} (2 × C≡O); MS (70 eV, EI): *m/z* (%): 609 (3) [M^+], 581 (1) [M^+–CO], 553 (4) [M^+–2CO]. 528 (5) [M^+–HBr], 472 (33) [M^+–2CO–Br], 345 (12) [M^+–2CO–$P\{OCH(CH_3)_2\}_3$], 209 (100) [$P\{OCH(CH_3)_2\}_3^+$]; $C_{20}H_{43}BrFeO_8P_2$ (609.3) calcd C 39.43, H 7.11, Br 13.11, Fe 9.17; found C 39.64, H 7.31, Br 12.98, Fe 9.70.

12a,b were identified by comparison with reported spectroscopic data [13].

12a: Yield: 0.37 g (86%). ^1H NMR (C_6D_6, r.t.): δ = –6.26 (t, J_{PH} = 51.5, Fe*H*), 1.00 (dt, J_{HH} = 7.6, J_{PH} = 15.2, CH_2CH_3), 1.64–1.76 (m, diastereotopic CH_2CH_3), 1.81–1.93 (m, diastereotopic CH_2CH_3); $^{13}C\{^1H\}$ NMR (C_6D_6, r.t.): δ = 7.6 (s, CH_2CH_3), 19.5 (t, J_{PC} = 13.9 Hz, CH_2CH_3), 211.0 (t, J_{PC} = 12.6 *CO*), 217.9 (t, J_{PC} = 25.2, *CO*); $^{31}P\{^1H\}$ NMR (C_6D_6, r.t.): δ = 50.4; IR (hexane): $\tilde{\nu}$ = 2001, 1940 cm^{-1} (2 × C≡O); MS (70 eV, EI): *m/z* (%): 428 (< 1) [M^+], 400 [M^+–CO], 371 [M^+–2CO–H], 320 [M^+–CO–HBr], 292 [M^+–2CO–HBr], 118 (100) [PEt_3^+].

12b: Yield: 0.42 g (88%). ^1H NMR (C_6D_6, r.t.): δ –7.10 (t, J_{PH} = 50.6 Fe*H*), 0.95 (dt, J_{HH} = 7.6, J_{PH} = 15.4, CH_2CH_3), 1.67–1.81 (m, diastereotopic CH_2CH_3), 1.89–2.04 (m, diastereotopic CH_2CH_3); $^{13}C\{^1H\}$ NMR (C_6D_6, r.t.): δ = 12.6 (s, CH_2CH_3), 25.4 (t, J_{PC} = 13.6 Hz, CH_2CH_3), 207.8 [t, J_{PC} = 12.4 *CO*], 215.0 (t, J_{PC} = 24.1, *CO*); $^{31}P\{^1H\}$ NMR (C_6D_6, r.t.): δ = 47.6; IR (hexane): $\tilde{\nu}$ = 1998, 1940 cm^{-1} (2 × C≡O); MS (70 eV, EI): *m/z* (%): 476 (4) [M^+], 448 [M^+–CO], 419 [M^+–2CO–H], 320 [M^+–CO–HI], 301 [M^+–2CO–H–PEt_3], 292 [M^+–2CO–HI^+], 118 (100) [PEt_3^+].

Preparation of dicarbonyl(dinitrogen)bis(triisopropylphosphite)iron (13), dicarbonyl(dinitrogen)bis(triethylphosphane)iron (14) and bis[dicarbonylbis(triethylphosphane)iron](μ-dinitrogen) (15): Since **13**–**15** are extremely labile at r.t., even in the solid state, we were not able to obtain correct chemical analyses for these complexes (fast decomposition is indicated by color change from yellow to brown).

$[Fe(CO)_2\{P(OiPr)_3\}_2Br_2]$ (**2a**) or $[Fe(CO)_2(PEt_3)_2X_2]$ (X = Br, I, **3a,b**) (1.5 mmol) in THF (100 mL) was stirred with sodium amalgam (≤1%, ca. 10 mmol Na) at –25 °C under 1 atm of N_2. After 2–3 h (IR monitoring) the supernatant suspension was transferred to a frit through a canula. Cold filtration through Celite was followed by evaporation of the filtrate to dryness in vacuo at ≤–20 °C.

$[Fe(CO)_2\{P(OiPr)_3\}_2N_2]$ (13): Extraction with hexane, filtration over Celite, concentration of the solution, and crystallization at –80 °C yielded 0.48 g (57%) of **13** as a yellow powder. ^1H NMR ([D_8]toluene, –20 °C): δ = 1.27 (d, J_{HH} = 5.7, $CH(CH_3)_3$), 4.85 (sept, J_{HH} = 5.7, $CH(CH_3)_3$); $^{13}C\{^1H\}$ NMR ([D_8]toluene, –20 °C): δ = 24.0 (s, $CH(CH_3)_3$), 69.7 (s, $CH(CH_3)_3$), 213.1 (t, J_{PC} = 44.9, *CO*); $^{31}P\{^1H\}$ NMR ([D_8]THF, –20 °C): δ = 185.4; $^{15}N\{^1H\}$ NMR ([D_8]THF, –40 °C): δ = –69.4 (dt, J_{NN} = 3.3, J_{PN} = 6.3, N_α), –40.6 (d, J_{NN} = 3.3, N_β); IR (THF): $\tilde{\nu}$ = 2141 (N≡N), 1924, 1886 cm^{-1} (2 × C≡O), IR (hexane): $\tilde{\nu}$ = 2147 (N≡N), 1928, 1872 cm^{-1} (2 × C≡O).

$[Fe(CO)_2(PEt_3)_2N_2]$ (14): **3b** could also be reduced with Na/Hg in ether under the same conditions as described above. Cold pentane was added directly to the yellow-orange ether filtrate. This induced precipitation of a ca. 1:1 mixture of **14** (orange crystals) and **15** (yellow crystals) at –80 °C. Repeated attempts to isolate **14** by fractional crystallization were unsuccessful. Combined yield of **14** and **15**: 0.41 g (73%). **14**: ^1H NMR ([D_8]toluene, –20 °C): δ = 1.02 (dt, J_{HH} = 7.5, J_{PH} = 14.7, CH_2CH_3), 1.47 (m, CH_2CH_3); $^{13}C\{^1H\}$ NMR ([D_8]THF, –10 °C): δ = 8.1 (m, CH_2CH_3), 20.9 (t, J_{PC} = 13 Hz, CH_2CH_3), 214.9 (t, J_{PC} = 33 Hz, *CO*); $^{31}P\{^1H\}$ NMR ([D_8]THF, 10 °C): δ = 66.5 (s); $^{15}N\{^1H\}$ NMR ([D_8]THF, –10 °C): δ = –62.1 (m, N_α), –39.7 (m, N_β); IR (THF): $\tilde{\nu}$ = 2097 cm^{-1} (N≡N), $\tilde{\nu}$ = 1897 cm^{-1}, 1849 cm^{-1} (2 × C≡O), IR (hexane): $\tilde{\nu}$ = 2098 (N≡N), $\tilde{\nu}$ = 1899, 1849 cm^{-1} (2 × C≡O).

Table 4. Data collection and processing parameters of **5a**, **6b**, **14**, and **15**.

	5a	**6b**	**14**	**15**
formula	$C_{20}H_{42}FeBrO_8P_2$	$C_{14}H_{30}FeIO_2P_2$	$C_{14}H_{30}FeN_2O_2P_2$	$C_{28}H_{60}Fe_2N_2O_4P_4$
M_r	608.2	475.1	376.2	724.4
color and habit	blue plate	black prism	yellow plate	yellow prism
crystal dimensions	0.20 × 0.30 × 0.50	0.70 × 0.50 × 0.40	0.24 × 0.20 × 0.08	0.30 × 0.15 × 0.08
crystal system	triclinic	tetragonal	orthorombic	monoclinic
space group	$P\bar{1}$	$P4_12_12$	*Pbca*	*C*2/c
a, Å	8.477(4)	8.259(2)	11.248(6)	20.220(8)
b, Å	12.226(6)		13.838(4)	12.849(5)
c, Å	16.739(10)	30.326(9)	26.234(9)	17.697(7)
α, deg	70.28(2)			
β, deg	79.78(2)			123.36(3)
γ, deg	72.51(2)			
V, Å^3	1552.0(14)	2068.6(10)	4083(3)	3840(3)
Z	2	4	8	8
ρ_{calcd}, g cm^{-1}	1.301	1.525	1.224	1.253
$2\theta_{max}$	54	58	52	56
scan mode	ω	ω	ω–2θ	ω–2θ
T, °C	–70	25	–60	–60
scan speed, deg min^{-1}	variable; 5.33–29.3	variable; 3.97–14.65	variable; 2.00–14.65	variable; 2.00–14.65
scan width	1.40	1.20	2.20	1.70
collection range	$+h, \pm k, \pm l$	$+h, +k, +l$	$+h, +k, +l$	$+h, +k, \pm l$
no. of measured refl.	7028	2961	4005	4945
no. of independent refl.	6510	2591	4005	4449
no. of refl. refined	4239	1855	1049	1873
σ limits	$F > 4.0\sigma(F)$	$F \geq 6\sigma(F)$	$F \geq 4\sigma(F)$	$F \geq 6\sigma(F)$
μ, cm^{-1}	19.11	23.58	9.00	9.49
no. of parameters	289	90	190	183
weighting scheme	$w^{-1} = \sigma^2(F) + 0.0003F^2$	unit weights	$w^{-1} = \sigma^2(F) + 0.0041F^2$	$w^{-1} = \sigma^2(F) + 0.0005F^2$
$R\|F\|$	0.057	0.046	0.092	0.089
$R_w\|F\|$	0.062	0.047	0.101	0.103
resid. elec. density, e Å^{-3}	1.21 to –0.91	0.73 to –1.13	0.68 to –0.59	0.82 to –1.23

[{Fe(CO)$_2$(PEt$_3$)$_2$}$_2$(μ-N$_2$)] (15): Two careful recrystallizations from ether at $-80\,^{\circ}C$ yielded yellow crystals. Yield: 0.32 g (58%). ^{1}H NMR ([D$_8$]toluene, $-90\,^{\circ}C$): $\delta = 1.06$ (s br, CH_2CH_3), 1.55 (s br, CH_2CH_3); $^{13}C\{^1H\}$ NMR ([D$_8$]THF, $-20\,^{\circ}C$): $\delta = 8.3$ (m, CH_2CH_3), 20.6 (t, $J_{PC} = 14$, CH_2), 216.1 (t, $J_{PC} = 33$, CO); $^{31}P\{^1H\}$ NMR ([D$_8$]toluene, $-90\,^{\circ}C$): $\delta = 65.4$; IR (fluorolube): $\tilde{\nu} = 2022$, 1966, 1879 cm^{-1} (3 × C=O).

X-ray Crystal Structure Determinations of 5a, 6b, 14, and 15: A single crystal of **5a** was mounted under nitrogen on a glass fiber by using a highly viscous perfluoropolyether, which was frozen at $-70\,^{\circ}C$. A crystal of **6b** was mounted on a glass fiber by using 5 min epoxy resin. Single crystals of thermally labile **14** and **15** were transferred under nitrogen onto the goniostat at $-60\,^{\circ}C$. The unit cells were determined and refined from 24 equivalent reflections with $2\theta \geq 24-28°$, obtained on a Siemens R3m/v four-circle diffractometer ($Mo_{K\alpha}$, $\lambda = 0.71073$ Å). Intensity data were collected and corrected for Lorentz and polarization effects, but not for absorption. Three reflections were monitored periodically for each compound as a check for crystal decomposition or movement. No significant variations in these standards were observed; therefore no correction was applied. Backgrounds were scanned for 25% of the peak widths on each end of the scans. Owing to the low quality of the crystals of the thermally labile complexes **14** and **15**, the number of reflections applicable to structure solution and refinement were restricted. The two Fe centers and the μ-N$_2$ ligand in **15** were located on special positions, namely, on (two-fold) axes in space group $C2/c$. All structures were solved by direct methods, from which the heavy atoms were located. The other non-hydrogen atoms were found in subsequent difference Fourier maps. Anisotropic refinement was applied for all non-hydrogen atoms. In the structures of **5a**, **6b**, **14**, and **15** the H atoms were generated geometrically (C–H bonds fixed at 0.96 Å). The isotropic temperature factor of $U = 0.08$ Å^2 was assigned to all H atoms. Computations were performed with the SHELXTL PLUS program package [29] on a VAX station 3100 (for **6b** and **15**) or on a 486IBM PC computer (for **5a** and **14**). Details of crystal parameters, data collection, and structure refinement are given in Table 4. Selected bond lengths and angles are listed in Tables 2 and 3. Tables of structure determination summaries, lists of anisotropic displacement parameters, lists of atom coordinates, and full lists of bond lengths and angles have been deposited [30].

EHT calculations [8]: The following bond lengths and angles were used in the calculation on [Fe(CO)$_2$(PH$_3$)$_2$X]: Fe–C = 1.77, Fe–P = 2.25, P–H = 1.40, C–O = 1.14, Fe–I = 2.60, and Fe–Br = 2.42 Å; P-Fe-P = 180, P-Fe-I·Br = 90°. The atomic orbital parameters were standard ones from CACAO [8], except for the iron atoms: s $H_{ii} = -8.86$ eV, $c = 1.90$; p $H_{ii} = -5.12$ eV, $c = 1.90$; d $H_{ii} = -12.2$ eV, $c_1 = 5.35$, $c_2 = 1.80$, $\xi_1 = 0.5366$, $\xi_2 = 0.6678$.

Acknowledgement: Financial support from the Swiss National Science Foundation is gratefully acknowledged. We thank Priv.-Doz. Dr. E. Roduner, Physikalisch-Chemisches Institut, Universität Zürich, for helpful discussions on the EPR spectra and are grateful to Prof. W. Herrmann and M. Barth, Anorganisch-Chemisches Institut der Technischen Universität München, Germany, for providing us with elemental analyses of the complexes **5a,b** and **6a,b**.

Received: March 2, 1995 [F96]

[1] a) J. K. Kochi, in *Organometallic Mechanisms and Catalysis*, Academic Press, New York, **1978**; b) W. C. Trogler, *Organometallic Radical Processes*; 1st ed., Elsevier, Amsterdam, **1990**, Vol. 22; c) C. Amatore, A. Jutand, *Organometallics* **1988**, *7*, 2203–2214; d) C. Amatore, M. Azzabi, A. Jutand, *J. Organomet. Chem.* **1989**, *363*, C41–45.

[2] a) G. Cardaci, G. Bellachioma, P. Zanazzi, *Organometallics* **1988**, *7*, 172–180; b) S. Komiya, M. Akita, A. Yoza, N. Kasuga, A. Fukuoka, Y. Kai, *J. Chem. Soc. Chem. Commun.* **1993**, 787–788; c) M. Antberg, L. Dahlenburg, *Z. Naturforsch.* **1987**, *42b*, 435–440; d) W. Hieber, J. Muschi, *Chem. Ber.* **1965**, *98*, 3931–3936.

[3] a) H. Berke, G. Huttner, W. Bankhardt, J. von Seyerl, L. Zsolnai, *Chem. Ber.* **1981**, *114*, 2754–2768; b) R. Birk, U. Grössmann, H.-U. Hund, H. Berke, *J. Organomet. Chem.* **1988**, *345*, 321–329.

[4] a) R. Birk, H. Berke, G. Huttner, L. Zsolnai, *Chem. Ber.* **1988**, *121*, 1557–1564; b) R. Birk, H. Berke, H.-U. Hund, G. Huttner, L. Zsolnai, L. Dahlenburg, U. Behrens, T. Sielisch, *J. Organomet. Chem.* **1989**, *372*, 397–410; c) R. Birk, H. Berke, G. Huttner, L. Zsolnai, *Chem. Ber.* **1988**, *121*, 471–476.

[5] A. G. Orpen, L. Brammer, F. H. Allen, O. Kennard, D. G. Watson, R. Taylor, *J. Chem. Soc. Dalton Trans.* **1989**, S1–83.

[6] a) A. Begum, A. R. Lyons, M. C. R. Symons, *J. Chem. Soc. A* **1971**, 2290–2293; b) M. Iwaizumi, T. Kishi, T. Isobe, F. Watari, *J. Chem. Soc. Faraday Trans. II* **1976**, *72*, 113–117.

[7] a) J. H. MacNeil, A. C. Chiverton, S. Fortier, M. C. Baird, R. C. Hynes, A. J. Williams, K. F. Preston, T. Ziegler, *J. Am. Chem. Soc.* **1991**, *113*, 9834–9842; b) W. C. Trogler, M. J. Therien, *J. Am. Chem. Soc.* **1986**, *108*, 3697–3702; c) P. K. Baker, N. G. Connelly, B. M. R. Jones, J. P. Maher, K. R. Somers, *J. Chem. Soc. Dalton Trans.* **1980**, 579–585.

[8] C. Mealli, D. M. Proserpio, *J. Chem. Educ.* **1990**, *67*, 399–402.

[9] a) P. Krusic, W. J. Cote, A. Grand, *J. Am. Chem. Soc.* **1984**, *106*, 4642–4643; b) P. Krusic, D. J. Jones, D. C. Roe, *Organometallics* **1986**, *5*, 456–460.

[10] B. De Klerk-Engels, J. H. Groen, M. J. A. Kraakman, J. M. Ernsting, K. Vrieze, K. Goubitz, J. Fraanje, *Organometallics* **1994**, *13*, 3279–3292.

[11] a) X.-X. Zhang, B. B. Wayland, *J. Am. Chem. Soc.* **1994**, *116*, 7897–7898; b) C. Bianchini, F. Laschi, M. Peruzzini, P. Zanello, *Gazz. Chim. Ital.* **1994**, *124*, 271–274; c) S. J. Sherlock, D. C. Boyd, B. Moasser, W. L. Gladfelter, *Inorg. Chem.* **1991**, *30*, 3626–3632; d) L. S. Crocker, D. M. Heinekey, G. K. Schulte, *J. Am. Chem. Soc.* **1989**, *111*, 405–406.

[12] R. F. Lang, R. D. Ju, G. Kiss, C. D. Hoff, J. C. Bryan, G. J. Kubas, J. *Am. Chem. Soc.* **1994**, *116*, 7917–7918.

[13] M. Jänicke, Ph.D. Thesis, University of Zürich, **1993**.

[14] H.-Y. Lin, K. Eriks, A. Prock, W. P. Giering, *Organometallics* **1990**, *9*, 1758–1766.

[15] a) D. C. Busby, T. A. George, S. D. A. Iske, S. D. Wagner, *Inorg. Chem.*, **1981**, *20*, 22–27; b) R. A. Henderson, G. J. Leigh, C. J. Pickett, *Adv. Inorg. Chem. Radiochem.* **1983**, *27*, 197–292.

[16] E. Gutiérrez, A. Monge, M. C. Nicasio, M. L. Poveda, E. Carmona, *J. Am. Chem. Soc.* **1994**, *116*, 791–792.

[17] a) C. A. Ghilardi, S. Midollini, L. Sacconi, P. Stoppioni, *J. Organomet. Chem.* **1981**, *205*, 193–202; b) I. R. Buys, L. D. Field, T. W. Hambley, A. E. D. Mc Queen, *Acta Crystallogr.* **1993**, *C49*, 1056–1059; c) A. Hills, D. L. Hughes, M. Jimenez-Tenorio, G. J. Leigh, *J. Organomet. Chem.* **1990**, *391*, C41–C44; d) S. Komiya, M. Akita, N. Kasuga, M. Hirano, A. Fukuoka, *J. Chem. Soc. Chem. Commun.* **1994**, 1115–1116.

[18] a) G. J. Leigh, M. J. Tenorio, *J. Am. Chem. Soc.*, **1991**, *113*, 5862–5863; b) R. A. Cable, M. Green, R. E. Mackenzie, P. L. Timms, T. W. Turney, *J. Chem. Soc. Chem. Commun.* **1976**, 270–271.

[19] R. Müller, J. D. Wallis, W. von Philipsborn, *Angew. Chem. Int. Ed. Engl.* **1985**, *24*, 513–515.

[20] R. Boča, *Chem. Listy* **1988**, *82*, 578–605.

[21] a) K. Nakamoto, *Infrared and Raman Spectra of Inorganic and Coordination Compounds*, John Wiley, New York, **1978**; b) D. A. Adams, *Metal–Ligand and Related Vibrations*, Edward Arnold, London, **1966**.

[22] C. Bianchini, F. Laschi, D. Masi, F. M. Ottaviani, A. Pastor, M. Peruzzini, P. Zanello, F. Zanobini, *J. Am. Chem. Soc.* **1993**, *115*, 2723–2730.

[23] M. Rosi, A. Segamelotti, F. Tarantelli, C. Floriani, L. S. Cederbaum, *J. Chem. Soc. Dalton Trans.* **1989**, 33–38.

[24] a) F. Bottomley, S. C. Nyburg, *J. Chem. Soc. Chem. Commun.* **1966**, 897–898; b) F. Bottomley, S. C. Nyburg, *Acta Cryst.* **1968**, *B24*, 1289–1293.

[25] D. M. Treitel, M. T. Flood, R. E. Marsh, H. B. Gray, *J. Am. Chem. Soc.* **1969**, *91*, 6512–6513.

[26] R. L. Keiter, E. A. Keiter, K. H. Hecker, C. A. Boecker, *Organometallics* **1988**, *7*, 2466–2469.

[27] R. A. Hendersen, *Transition Met. Chem.* **1990**, *15*, 330–336.

[28] a) E. T. Libbey, M. Bancroft, *J. Chem. Soc. Dalton Trans.* **1974**, 87–92; b) M. Pankowski, M. Bigorgne, *J. Organomet. Chem.* **1977**, *125*, 231–252.

[29] G. M. Sheldrick, *SHELXTL-Plus*, **1990**, *Release 4.2*, Siemens Analytical X-ray Instruments, Madison, USA.

[30] Further details of the crystal structure investigation may be obtained from the Fachinformationszentrum Karlsruhe, D-76344 Eggenstein-Leopoldshafen (Germany), on quoting the depository number CSD-59091.